

Overcoming the Paradox of Certified Training with Gaussian Smoothing

Stefan Balauca¹ Mark Niklas Müller² Yuhao Mao² Maximilian Baader² Marc Fischer² Martin Vechev²

Abstract

Training neural networks with high certified accuracy against adversarial examples remains an open problem despite significant efforts. While certification methods can effectively leverage tight convex relaxations for bound computation, in training, these methods perform worse than looser relaxations. Prior work hypothesized that this is caused by the discontinuity and perturbation sensitivity of the loss surface induced by these tighter relaxations. In this work, we show theoretically that Gaussian Loss Smoothing can alleviate both of these issues. We confirm this empirically by proposing a certified training method combining PGPE, an algorithm computing gradients of a smoothed loss, with different convex relaxations. When using this training method, we observe that tighter bounds indeed lead to strictly better networks that can outperform state-of-the-art methods on the same network. While scaling PGPE-based training remains challenging due to high computational cost, our results clearly demonstrate the promise of Gaussian Loss Smoothing for training certifiably robust neural networks.

1. Introduction

The increased deployment of deep learning systems in mission-critical applications has made their provable trustworthiness and robustness against adversarial examples (Biggio et al., 2013; Szegedy et al., 2014) an important topic. As state-of-the-art neural network certification has converged to increasingly similar approaches (Zhang et al., 2022; Ferrari et al., 2022), the focus in the field is now shifting to specialized training methods that yield networks with high certified robustness while minimizing the loss of standard accuracy (Müller et al., 2023; Palma et al., 2023).

¹INSAIT, Sofia University, Sofia, Bulgaria ²Department of Computer Science, ETH Zürich, Switzerland. Correspondence to: Stefan Balauca <stefan.balauca@insait.ai>.

Relaxation	Tightness	GRAD		PGPE
IBP	0.55	91.23	Loss Smoothing ⇒	87.02
CROWN-IBP	1.68	88.76		90.23
DEEPPOLY	2.93	90.04		91.53

Figure 1. Illustration of how Gaussian loss smoothing overcomes the paradox of certified training. We compare the certified accuracy [%] obtained by training with different relaxations using either the standard gradient (GRAD) or a gradient estimate computed on the smoothed loss surface (PGPE) with the tightness of the method.

Certified Training State-of-the-art certified training methods aim to optimize the network’s worst-case loss over an input region defined by an adversarial specification. However, as computing the exact worst-case loss is NP-complete (Katz et al., 2017), they typically utilize convex relaxations to compute over-approximations (Gowal et al., 2018; Singh et al., 2018; 2019). Surprisingly, training methods based on the least precise relaxations (IBP) empirically yield the best performance (Shi et al., 2021), while tighter relaxations perform progressively worse (left-hand side of Figure 1). Jovanović et al. (2022) investigated this surprising phenomenon which they call the “Paradox of Certified Training”, both theoretically and empirically and found that tighter relaxations induce harder optimization problems. Specifically, they identify the *continuity* and *sensitivity* of the loss surface induced by a relaxation as key factors for the success of certified training, beyond its *tightness*. Indeed, *all* state-of-the-art methods are based on the imprecise but continuous and insensitive IBP bounds (Müller et al., 2023; Mao et al., 2023a; Palma et al., 2023). However, while these IBP-based methods improve robustness, they induce severe regularization, significantly limiting the effective capacity and thus standard accuracy (Mao et al., 2023b). Overall, this raises the following fundamental question:

Can the paradox of certified training and thus the robustness-accuracy trade-off be overcome?

This Work: Overcoming the Paradox We investigate this question and show that applying *Gaussian Loss Smoothing* to certified training induces both continuity and infinite differentiability by smoothing the worst-case loss approximation with a Gaussian kernel. Leveraging this insight we propose the first backpropagation-free certified training method, recovering Gaussian Loss Smoothing in expecta-

tion, based on PGPE (Sehnke et al., 2010). We demonstrate empirically that using this method, tighter relaxations indeed lead to strictly better networks, thereby both confirming the importance of continuity and sensitivity in the paradox of certified training and overcoming it (right-hand side of Figure 1). Combining PGPE with the precise DEEPPOLY relaxation (Singh et al., 2019), we obtain strictly better results than IBP with gradient-based optimization across all settings and even outperform state-of-the-art methods on the same networks. While scaling PGPE-based training remains challenging due to its high computational cost, we believe that our results clearly demonstrate the promise of Gaussian Loss Smoothing for certified training, suggesting fruitful directions for future work.

Main Contributions Our core contributions are:

- We theoretically investigate the effect of Gaussian Loss Smoothing on the continuity and sensitivity of the approximate worst-case loss in certified training.
- Based on these insights, we propose a novel PGPE-based certified training method that achieves the tightness of DeepPoly bounds while ensuring continuity via Gaussian Loss Smoothing.
- We conduct a large-scale empirical evaluation of different convex relaxations under PGPE optimization, requiring over 100,000 GPU hours, and demonstrating the promise of Loss Smoothing based approaches.

2. Training for Certified Robustness

Below, we first introduce our notation and the setting of adversarial robustness before providing a background on (training for) certified robustness.

Notation We denote vectors with bold lower-case letters $\mathbf{a} \in \mathbb{R}^n$, matrices with bold upper-case letters $\mathbf{A} \in \mathbb{R}^{n \times d}$, and sets with upper-case calligraphic letters $\mathcal{A} \subset \mathbb{R}$. All inequalities $\mathbf{a} \geq \mathbf{b}$ between vectors hold elementwise.

2.1. Adversarial Robustness

We consider a neural network $\mathbf{f}_\theta(\mathbf{x}): \mathcal{X} \rightarrow \mathbb{R}^n$, parameterized by the weights θ , that assigns a score to each class $i \in \mathcal{Y}$ given an input $\mathbf{x} \in \mathcal{X}$. This induces the classifier $F: \mathcal{X} \rightarrow \mathcal{Y}$ as $F(\mathbf{x}) := \arg \max_i \mathbf{f}_\theta(\mathbf{x})_i$. We call F locally robust for an input $\mathbf{x} \in \mathcal{X}$ if it predicts the same class $y \in \mathcal{Y}$ for all inputs in an ϵ -neighborhood $\mathcal{B}_p^\epsilon(\mathbf{x}) := \{\mathbf{x}' \in \mathcal{X} \mid \|\mathbf{x} - \mathbf{x}'\|_p \leq \epsilon\}$. To prove that a classifier is locally robust, we thus have to show that $F(\mathbf{x}') = F(\mathbf{x}) = y, \forall \mathbf{x}' \in \mathcal{B}$.

Local robustness is equivalent to the score of the target class y being greater than that of all other classes for all

relevant inputs, i.e., $\min_{\mathbf{x}' \in \mathcal{B}, i \neq y} \mathbf{f}_\theta(\mathbf{x}')_y - \mathbf{f}_\theta(\mathbf{x}')_i > 0$. As solving this neural network verification problem exactly is generally NP-complete (Katz et al., 2017), state-of-the-art neural network verifiers relax it to an efficiently solvable convex optimization problem (Brix et al., 2023). To this end, the non-linear activation functions are replaced with convex relaxations in their input-output space, allowing linear bounds of the following form on their output $\mathbf{f}(\mathbf{x})$ to be computed:

$$\mathbf{A}_l \mathbf{x} + \mathbf{b}_l \leq \mathbf{f}_\theta(\mathbf{x}) \leq \mathbf{A}_u \mathbf{x} + \mathbf{b}_u,$$

for some input region $\mathcal{B}_p^\epsilon(\mathbf{x})$. These bounds can in-turn be bounded concretely by $\mathbf{l}_y = \min_{\mathbf{x} \in \mathcal{B}} \mathbf{A}_{l_i} \mathbf{x} + \mathbf{b}_{l_i} \in \mathbb{R}$ and \mathbf{u}_y analogously. Hence, we have $\mathbf{l}_y \leq \mathbf{f}(\mathbf{x}) \leq \mathbf{u}_y$.

Training for Robustness To obtain (certifiably) robust neural networks, specialized training methods are required. For a data distribution $(\mathbf{x}, t) \sim \mathcal{D}$, standard training optimizes the network parametrization θ to minimize the expected cross-entropy loss:

$$\theta_{\text{std}} = \arg \min_{\theta} \mathbb{E}_{\mathcal{D}} [\mathcal{L}_{\text{CE}}(\mathbf{f}_\theta(\mathbf{x}), t)], \quad \text{with} \quad (1)$$

$$\mathcal{L}_{\text{CE}}(\mathbf{y}, t) = \ln \left(1 + \sum_{i \neq t} \exp(y_i - y_t) \right). \quad (2)$$

To train for robustness, we, instead, aim to minimize the expected *worst-case loss* for a given robustness specification, leading to a min-max optimization problem:

$$\theta_{\text{rob}} = \arg \min_{\theta} \mathbb{E}_{\mathcal{D}} \left[\max_{\mathbf{x}' \in \mathcal{B}^\epsilon(\mathbf{x})} \mathcal{L}_{\text{CE}}(\mathbf{f}_\theta(\mathbf{x}'), t) \right]. \quad (3)$$

As computing the worst-case loss by solving the inner maximization problem is generally intractable, it is commonly under- or over-approximated, yielding adversarial and certified training, respectively.

Adversarial Training optimizes a lower bound on the inner optimization objective in Equation (3). To this end, it first computes concrete examples $\mathbf{x}' \in \mathcal{B}^\epsilon(\mathbf{x})$ that approximately maximize the loss term \mathcal{L}_{CE} and then optimizes the network parameters θ for these examples. While networks trained this way typically exhibit good empirical robustness, they remain hard to formally certify and are sometimes vulnerable to stronger attacks (Tramèr et al., 2020; Croce & Hein, 2020).

Certified Training typically optimizes an upper bound on the inner maximization objective in Equation (3). To this end, the robust cross-entropy loss $\mathcal{L}_{\text{CE,rob}}(\mathcal{B}^\epsilon(\mathbf{x}), t) = \mathcal{L}_{\text{CE}}(\bar{\mathbf{y}}^\Delta, t)$ is computed from an upper bound $\bar{\mathbf{y}}^\Delta$ on the logit differences $\mathbf{y}^\Delta := \mathbf{y} - y_t$ obtained via convex relaxations as described above and then plugged into the standard cross-entropy loss.

As this can induce strong over-regularization if the used convex relaxations are imprecise and thereby severely reduce the standard accuracy of the resulting models, current state-of-the-art certified training methods combine these bounds with adversarial training (Palma et al., 2022; Müller et al., 2023; Mao et al., 2023a; Palma et al., 2023). We now introduce the convex relaxations popular for neural networks.

2.2. Convex Relaxations

We now discuss four popular convex relaxations of different precision, which we investigate in this work.

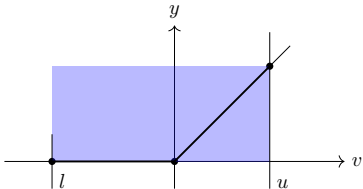


Figure 2. IBP-relaxation of a ReLU with an input $v \in [l, u]$.

IBP Interval bound propagation (Mirman et al., 2018; Gehr et al., 2018; Gowal et al., 2018) only considers elementwise, constant bounds of the form $l \leq v \leq u$. Affine layers $y = Wv + b$ are thus also relaxed as

$$\frac{W(l+u) - |W|(u-l)}{2} + b \leq Wv + b \leq \frac{W(l+u) + |W|(u-l)}{2} + b,$$

where $|\cdot|$ is the elementwise absolute value. ReLU functions are relaxed by their concrete lower and upper bounds $\text{ReLU}(l) \leq \text{ReLU}(v) \leq \text{ReLU}(u)$, illustrated in Figure 2.

Hybrid Box (HBox) The HBox relaxation is an instance of Hybrid Zonotope (Mirman et al., 2018) which combines the exact encoding of affine transformations from the DEEPZ or Zonotope domain (Singh et al., 2018; Wong & Kolter, 2018; Weng et al., 2018; Wang et al., 2018) with the simple IBP relaxation of unstable ReLUs, illustrated in Figure 2. While less precise than DEEPZ, HBOX ensures constant instead of linear representation size in the network depth, making its computation much more efficient.

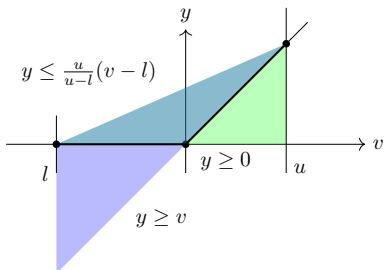


Figure 3. DEEPPOLY relaxation of a ReLU with bounded inputs $v \in [l, u]$. The lower-bound slope λ is chosen to minimize the area between the upper- and lower-bound in the input output space, resulting in the blue or green area.

DeepPoly (DP) DEEPPOLY, introduced by Singh et al. (2019), is mathematically identical to CROWN (Zhang et al., 2018) and based on recursively deriving linear bounds of the form

$$A_l x + a_l \leq v \leq A_u x + a_u$$

on the outputs of every layer. While this allows affine layers to be handled exactly, ReLU layers $y = \text{ReLU}(v)$ are relaxed neuron-wise, using one of the two relaxations illustrated in Figure 3:

$$\lambda v \leq \text{ReLU}(v) \leq (v - l) \frac{u}{u - l},$$

where product and division are elementwise. The lower-bound slope $\lambda = \mathbb{1}_{|u| > |l|}$ is chosen depending on the input bounds l and u to minimize the area between the upper- and lower-bound in the input-output space. Crucially, a minor change in the input bounds can thus lead to a large change in output bounds when using the DEEPPOLY relaxation.

CROWN-IBP To reduce the computational complexity of DEEPPOLY, CROWN-IBP (Zhang et al., 2020) uses the cheaper but less precise IBP bounds to compute the concrete upper- and lower-bounds u and l on ReLU inputs required to define the DEEPPOLY relaxation. To compute the final bounds on the network output DEEPPOLY is used. This reduces the computational complexity from quadratic to linear in the network depth. While, CROWN-IBP is not strictly more or less precise than either IBP or DEEPPOLY, its precision empirically lies between the two.

Relaxation Tightness While we rarely have strict orders in tightness (only HBOX is strictly tighter than IBP), we can compare the tightness of relaxations empirically given a network to analyze. Jovanović et al. (2022) propose to measure the tightness of a relaxation as the AUC score of its certified accuracy over perturbation radius curve. This metric implies the following empirical tightness ordering $\text{IBP} < \text{HBox} < \text{CROWN-IBP} < \text{DEEPPOLY}$ (Jovanović et al., 2022), which agrees well with our intuition.

2.3. The Paradox of Certified Training

The robustness-accuracy trade-off dominating certified training describes how strongly we need to regularize for (certifiable) robustness at the cost of reduced standard accuracy. Intuitively, one would expect more precise relaxations to induce weaker regularisation and thus better standard and possibly also better certified accuracy. However, empirically the least precise relaxation, IBP, dominates the more precise methods, e.g., DEEPPOLY, with respect to both certified and standard accuracy (see the left-hand side of Figure 1). This is all the more surprising given that state-of-the-art certified training methods introduce artificial unsoundness into these IBP bounds to improve tightness at the cost of soundness

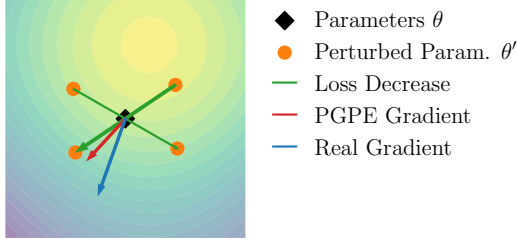


Figure 4. Illustration the PGPE algorithm: First we sample random perturbations around the central point from a Gaussian distribution with standard deviation σ_{PGPE} . Then we compute the loss difference between pairs of symmetric points. Finally, we estimate the gradient as a sum of sampled directions weighted by the magnitude of loss change in each direction.

to reduce regularisation and improve performance (Müller et al., 2023; Mao et al., 2023a; Palma et al., 2023).

To explain this paradox, Jovanović et al. (2022) show that these more precise relaxations induce loss landscapes suffering from discontinuities and high sensitivity, making it extraordinarily challenging for gradient-based optimization methods to find good optima. Thus the key challenge of certified training is to design a robust loss that combines tight bounds with a continuous and smooth loss landscape.

Next, we discuss these challenges and show how to overcome them.

3. Gaussian Loss Smoothing for Certified Training

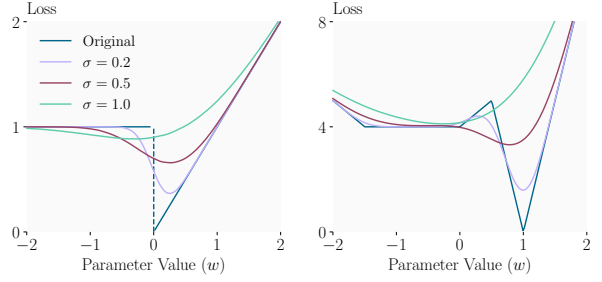
In this section, we first discuss Gaussian loss smoothing in policy gradient methods before showing how they can be applied to certified training. We defer the proofs to App. A.

3.1. Policy Gradients with Parameter-based Exploration

(PGPE) (Sehnke et al., 2010) is a gradient-free optimization algorithm that optimizes the Gaussian Smoothing loss $L_\sigma(\theta) := \mathbb{E}_{\theta' \sim \mathcal{N}(\theta, \sigma^2 \mathbf{I})} L(\mathbf{f}_{\theta'})$, where the loss is not evaluated at a single parameterization of the network, but rather at a (normal) distribution of parameterizations.

To this end, PGPE samples weight perturbation ϵ_i from $\mathcal{N}(0, \sigma_{\text{PGPE}}^2)$, and then evaluates the loss of the perturbed parametrizations $r_i^+ = L(\theta + \epsilon_i)$ and $r_i^- = L(\theta - \epsilon_i)$. These pairs of symmetric points are then used to compute gradient estimates with respect to both the mean of the weight distribution θ and its standard deviation σ_{PGPE} :

$$\begin{aligned} \nabla_{\theta} \hat{L}_\sigma(\theta) &\propto \sum_i \epsilon_i (r_i^+ - r_i^-), \\ \nabla_{\sigma_{\text{PGPE}}} \hat{L}_\sigma(\theta) &\propto \sum_i \left(\frac{r_i^+ + r_i^-}{2} - b \right) \left(\frac{\epsilon_i^2 - (\sigma_{\text{PGPE}})_i^2}{(\sigma_{\text{PGPE}})_i} \right), \end{aligned}$$



(a) Discontinuity.

(b) Sensitivity.

Figure 5. Illustrating the effect of Gaussian Loss Smoothing on the discontinuity (left) and sensitivity loss functions (right).

where b is a baseline computed from the mean of all $2n$ samples $b = \frac{1}{2n} \sum_i (r_i^+ + r_i^-)$. Figure 4 visualizes such a gradient estimate. In training, these gradients can be used to both update the mean weights θ and the main hyperparameter parameter of PGPE, the standard deviation σ_{PGPE} .

Indeed, PGPE recovers an unbiased estimate of the gradients on the Gaussian smoothed, see:

Lemma 3.1. *PGPE approximately minimizes the smoothed loss $L_\sigma(\theta)$ by sampling. In particular, the expectation of the PGPE update on θ is the true gradient of $L_\sigma(\theta)$, i.e., $\mathbb{E} \nabla_{\theta} \hat{L}_\sigma(\theta) = \nabla L_\sigma(\theta)$.*

As *no* backward propagation is needed to compute these gradient estimates, PGPE is comparable to neuro-evolution algorithms. In this context it is among the best performing methods for supervised learning (Lange et al., 2023).

Open Challenges: Discontinuity and Sensitivity We illustrate the key challenges causing the paradox of certified training (§2.3) on a toy network and loss in Figure 5.

On the left-hand side (original in Figure 5a), we show the DEEPPOLY lower bound of the one-neuron network $y = \text{ReLU}(x+w) + 1$ for $x \in [-1, 1]$ over the parameter w . As the original bound $l = 1 + \mathbb{1}_{w>0} \cdot (w-1)$ is discontinuous at $w = 0$, a gradient-based optimization method initialized at $w > 0$ will decrease w until it has moved through the discontinuity and past the local minimum.

The second key factor, sensitivity, can be interpreted as a combination of the number of local minima and the smoothness of the loss-landscape. Jovanović et al. (2022) show that DEEPPOLY is more sensitive than IBP, making it more likely that gradient-based optimization methods will get stuck in a bad local minimum. We illustrate this with the toy function shown in Figure 5b. There the original function has a bad local minimum for $w \in [-1.5, 0]$ that a gradient-based optimizer is likely to get stuck in.

We now discuss how Gaussian Loss Smoothing can address both of these challenges.

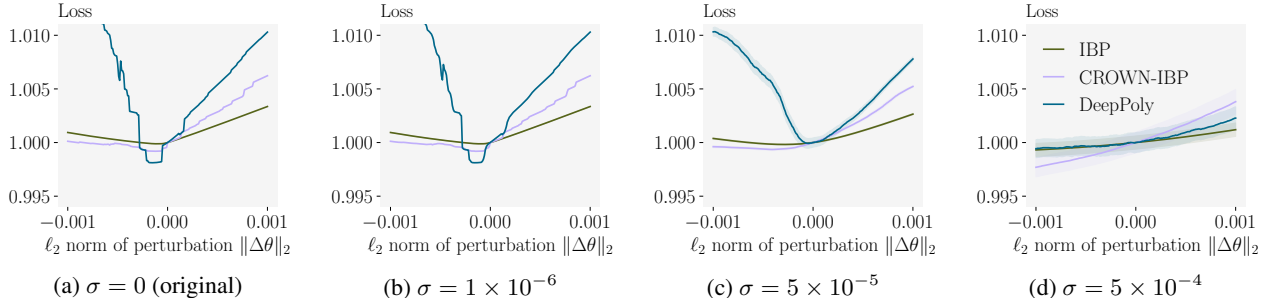


Figure 6. The original and Gaussian smoothed loss for different relaxations on a PGD-trained CNN3, evaluated along the direction of DEEPPOLY gradient. Losses are normalized by dividing them with the values at 0, i.e., without perturbation. The smoothed loss is estimated with 128 samples and the corresponding confidence interval is shown as shaded.

3.2. Gaussian Loss Smoothing for Certified Training

First, Gaussian Loss Smoothing (GLS) turns any discontinuous loss function (such as the one in Figure 5a) into a continuous one that is differentiable everywhere. More formally:

Corollary 3.2. *The loss surface under GLS is continuous, infinitely differentiable for any reasonably growing loss function $L(\theta)$.*

Second, Gaussian Smoothing can help to overcome the sensitivity issue. As we show in Figure 5b, depending on the standard deviation, the local minimum can be reduced or removed, and the loss landscape can be smoothed. However, the choice of standard deviation is crucial. While a too small standard deviation only has a minimal effect on loss smoothness and might not remove local minima, a too large standard deviation can oversmooth the loss, completely removing or misaligning minima. We again illustrate this in Figure 5b. There, a small standard deviation of $\sigma = 0.2$ does not smooth out the local minimum while a large standard deviation ($\sigma = 1.0$) severely misaligns the new global minimum with that of the original function. We again formalize this result in the following corollary.

Corollary 3.3. *The loss surface under GLS is L -smooth for any reasonably growing L -smooth loss function $L(\theta)$.*

We conclude that GLS has the potential to mitigate the key issues, discontinuity and sensitivity, identified by Jovanović et al. (2022) for tight bounding methods.

Empirical Confirmation To empirically confirm these effects, we plot the original and smoothed loss landscape (along the direction of the DEEPPOLY gradient) of different relaxations for a CNN3 and different standard deviations in Figure 6. We normalize all losses by dividing them by their value for the unperturbed weights.

We observe that the original loss (Figure 6a) is discontinuous and highly sensitive to perturbations for both CROWN-IBP and DEEPPOLY, consistent with the findings of Jovanović et al. (2022). Only the imprecise IBP loss is continuous

and smooth, explaining why the IBP loss is the basis for many successful certified training methods. When the loss is smoothed with small standard deviations $\sigma = 10^{-6}$ (Figure 6b), the local minimum of the DEEPPOLY loss has a slightly reduced sharpness but is still present. In addition, both the losses for DEEPPOLY and CROWN-IBP are still highly sensitive. This indicates a too small σ .

When the standard deviation is increased to $\sigma = 5 \cdot 10^{-5}$ (Figure 6c), the undesirable local minimum of the DEEPPOLY loss is removed completely, and both losses become much less sensitive to perturbations. However, further increasing the standard deviation to $\sigma = 5 \cdot 10^{-4}$ (Figure 6d), leads to almost flat losses removing the minimum present in the underlying loss.

These results empirically confirm the observations in our toy setting and predicted by our theoretical analysis, showing that Gaussian Loss Smoothing (via PGPE) mitigates the discontinuity and sensitivity issues formulated by Jovanović et al. (2022). Encouraged by these results, we now empirically evaluate the performance of PGPE-based certified training methods in the next section.

4. Experimental Evaluation

In this section, we rigorously evaluate the effect Gaussian Loss Smoothing via PGPE on the training characteristics of different bound computation methods.

First, we show in §4.1 that the “Paradox of Certified Training” (Jovanović et al., 2022) can be overcome by smoothing the loss surface, i.e., that under Gaussian Loss Smoothing training with tighter bounds will generally lead to better certified and standard accuracy.

Second, we investigate how the hyperparameters of PGPE affect the properties of the induced loss surface and thus interact with the performance of the resulting certified training method in §4.2.

Third and finally, we show in §4.3 that the effects outlined above become even more pronounced as we scale to deeper networks.

Experimental Setup We implement all certified training methods in PyTorch (Paszke et al., 2019) and conduct experiments on MNIST (LeCun et al., 2010) and CIFAR-10 (Krizhevsky et al., 2009) using l_∞ perturbations and modified versions of the CNN3 and CNN5 architectures (see Table 4 in App. B). For more details regarding experimental setting including all hyperparameters see App. B.

Standard Certified Training For standard certified training using back-propagation (referred to below as GRAD for clarity), use similar hyperparameters as recent work in this domain (Shi et al., 2021; Müller et al., 2023; Mao et al., 2023a) and initialize all models with Kaiming uniform (He et al., 2015). In particular, we also use the Adam optimizer (Kingma & Ba, 2015), follow their learning rate and ϵ -annealing schedule, use the same batch size and gradient clipping threshold, and use the same ϵ for training and certification. In the case of SABR and STAPS we conduct an extensive optimization of their network-specific hyperparameters and only report the best one.

PGPE Training We train our PGPE models using the multi-GPU, multi-actor implementation of `evotorch` (Toklu et al., 2023). As PGPE training is computationally expensive, we initialize from a PGD-trained model. This can be seen as a warm-up stage as is common also for other certified training methods (Shi et al., 2021; Müller et al., 2023; Mao et al., 2023a). We only use ϵ -annealing for the larger perturbation magnitudes on both MNIST and CIFAR-10 and choose learning-rate schedules based on a brief initial evaluation of training stability. Unless indicated otherwise, we run the PGPE algorithm with a population size of $n_{ps} = 256$ and an initial standard deviation for weight sampling of $\sigma_{PGPE} = 10^{-3}$.

Certification We use the state-of-the-art complete verification method MN-BAB (Ferrari et al., 2022) with the same settings as used by Müller et al. (2023) for all networks independently of the training method. We note that this is in contrast to Jovanović et al. (2022) who used the same method for training and verification. However, we aim to assess true robustness instead of certifiability with the same bounding method used during training.

Hardware For PGPE training, we used between 2 and 8 V100s or L4s. For standard certified training and certification, we used single A6000s or A100s. See App. B.5 for a detailed breakdown of the computational cost.

4.1. Overcoming the Paradox of Certified Training

In Table 1, we compare the performance of training with various convex relaxations using either backpropagation to calculate gradients directly (GRAD) or the PGPE algorithm to obtain estimates of the smoothed gradients.

GRAD Training We train the same CNN3 on MNIST and CIFAR-10 at the established perturbation magnitudes using standard certified training with IBP, HBOX, CROWN-IBP, and DEEPPOLY. We observe that across all these settings IBP dominates the other methods both in terms of standard and certified accuracy, agreeing well with the paradox of certified training. Among the remaining methods, HBOX, CROWN-IBP, and DEEPPOLY tend to perform similarly with CROWN-IBP being significantly better at MNIST $\epsilon = 0.3$, indicating that in the absence of continuity and for high sensitivity, tightness is less relevant.

PGPE Training Training the same CNN3 in the same settings with PGPE we observe that the performance ranking changes significantly (see Table 1). Now, training with the loose IBP bounds performs strictly worse than training with the more precise DEEPPOLY bounds across all datasets and perturbation sizes. In fact, the most precise DEEPPOLY bounds now yield the best certified accuracy across all settings, even outperforming GRAD-based training methods at low perturbation magnitudes.

Interestingly IBP still yields better certified accuracy at large perturbation magnitudes than HBOX and CROWN-IBP, although at significantly worse natural accuracies. This is likely due to the fact that a more severe regularization is required in these settings.

These results suggest that we were indeed able to alleviate the sensitivity and discontinuity problems of more precise convex relaxations by leveraging Gaussian Loss Smoothing. As Gaussian Loss Smoothing via PGPE does not require differentiability, this points to future training methods based on even more precise bounds than DEEPPOLY, computed, e.g., via a branch and bound-based procedure.

We note, that while DEEPPOLY + PGPE outperforms DEEPPOLY + GRAD in almost all settings and sometimes by a wide margin, it does not beat the state-of-the-art GRAD training methods in most settings. We believe this to be due to three key factors: First, PGPE computes a gradient approximation in an $\frac{n_{ps}}{2}$ -dimensional subspace. Thus, computing high-dimensional gradient information requires a population size corresponding to twice the number of network parameters. This, however, is computationally intractable even for the small networks we consider given the high cost of evaluating DEEPPOLY. Thus we only obtain low-dimensional gradient approximates, which lead to slower training (as we show in Table 2 and Figure 10). Second, again due to the high cost of training with PGPE, we used relatively short training schedules and were unable to optimize hyperparameters for the different settings. And third, PGPE-based certified training is less optimized, compared to standard certified training which has been extensively optimized over the past years (Shi et al., 2021; Müller et al., 2023; Palma et al., 2023).

Table 1. Comparison of the standard (Acc.) and certified (Cert. Acc.) accuracy for different certified training methods on the full MNIST and CIFAR-10. We use the state-of-the-art method MN-BAB (Ferrari et al., 2022) for certification.

Dataset	ϵ_∞	Relaxation	Nat. Acc. [%]		Cert. Acc. [%]		Adv. Acc. [%]			
			GRAD	PGPE	GRAD	PGPE	GRAD	PGPE		
MNIST	0.1	PGD	98.43	-	87.27	-	91.62	-		
		IBP	96.02	94.52	91.23	87.02	91.23	87.03		
		SABR	97.54	97.37	92.99	90.82	93.01	90.96		
		STAPS	97.48	96.31	93.53	89.39	93.53	89.41		
		HBOX	94.79	96.12	88.18	90.57	88.18	90.58		
		CROWN-IBP	94.33	96.69	88.76	90.23	88.77	90.25		
		DEEPPOLY	95.95	97.44	90.04	91.53	90.08	91.79		
	0.3	PGD	96.08	-	75.14	-	77.44	-		
		IBP	91.02	89.16	77.23	74.00	77.27	74.08		
		HBOX	83.75	86.58	57.86	70.52	57.92	70.66		
		CROWN-IBP	86.97	90.57	70.55	71.95	70.56	72.24		
		DEEPPOLY	77.87	91.05	47.28	74.28	47.36	74.98		
		CIFAR 10	2/255	PGD	60.35	-	34.62	-	40.12	-
				IBP	48.05	44.55	37.69	34.09	37.70	34.10
CROWN-IBP	44.49			51.19	35.75	37.51	35.75	37.65		
DEEPPOLY	47.70			54.17	36.72	38.95	36.72	40.20		
8/255	PGD		50.18	-	7.90	-	19.65	-		
	IBP		34.63	30.48	25.72	21.75	25.74	21.75		
	CROWN-IBP		31.60	32.36	22.66	21.40	22.66	21.42		
		DEEPPOLY	33.06	31.37	22.97	22.19	22.98	22.19		

Table 2. Effect of the population size n_{ps} on accuracy and training time with PGPE + DEEPPOLY training on CNN3.

Popsiz	Nat. [%]	Cert. [%]	GPU h
Init	97.14	94.02	-
64	97.22	94.07	88
128	97.22	94.13	160
256	97.30	94.19	304
512	97.27	94.22	596
1024	97.43	94.50	1192

4.2. Ablation Studies

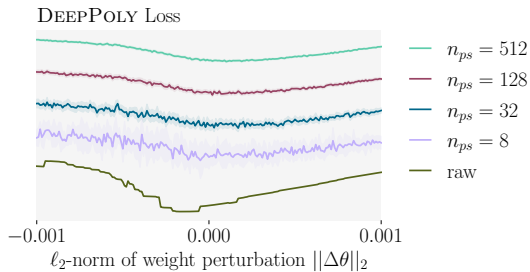


Figure 7. Effect of the population size n_{ps} on the induced loss surface in PGPE.

Population Size While PGPE recovers Gaussian Loss Smoothing in expectation, the quality of the gradient approximation depends strongly on the population size n_{ps} . In particular, a small population size n_{ps} induces a high-variance estimate of the true smoothed loss, leading to noisy gradient estimates and thus slow learning or even stability issues. We illustrate this in Figure 7 where we show the loss

surface along the gradient direction for different population sizes. We observe that for small population sizes the loss surface is indeed very noisy, only becoming visually smooth at $n_{ps} = 512$. Additionally, PGPE computes a gradient approximation in an $\frac{n_{ps}}{2}$ -dimensional subspace, thus further increasing gradient variance if n_{ps} is (too) small compared to the number of network parameters.

To assess the effect this has on the performance of PGPE training, we train the same CNN3 on MNIST using population sizes between 64 and 1024, presenting results in Table 2. We observe that performance does indeed improve significantly with increasing population sizes (note the relative performance compared to initialization). This becomes even more pronounced when considering the training dynamics (see Figure 10). Unfortunately, the computational cost of PGPE is significant and scales linearly in the population size. We thus choose $n_{ps} = 256$ for all of our main experiments, as this already leads to training times in excess of 3 weeks on 8 V100s for some experiments.

Standard Deviation The standard deviation σ used for Gaussian Loss Smoothing has a significant impact on the resulting loss surface as we illustrated in Figure 6 and discussed in §3. If σ is chosen too small, the loss surface will still exhibit high sensitivity and gradients will only be meaningful very locally as discontinuities are barely smoothed. On the other hand, if σ is chosen too large, the loss surface will become very flat and uninformative, preventing us from finding good solutions.

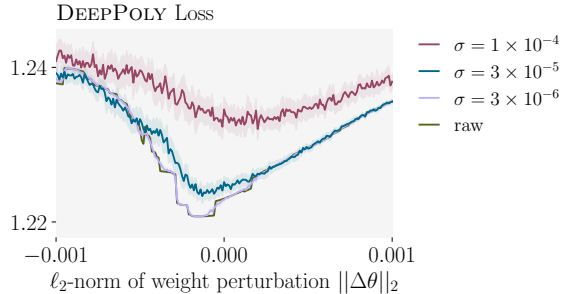


Figure 8. Effect of the standard deviation σ_{PGPE} on the induced loss surface in PGPE at a small population sizes of $n_{ps} = 32$.

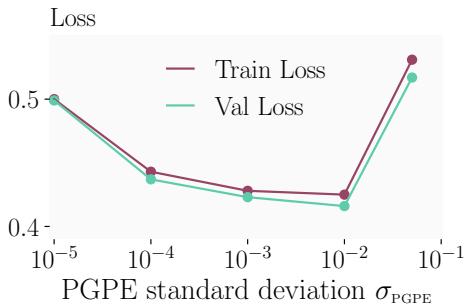


Figure 9. Train and Validation Losses after 50 epochs of training for different values of σ_{PGPE} .

When estimating the smoothed loss in PGPE via sampling at moderate population sizes n_{ps} , the standard deviation σ_{PGPE} additionally affects the variance of the loss and thus gradient estimate. We illustrate this in Figure 8, where we not only see the increasing large-scale smoothing effect discussed above but also an increasing level of small-scale noise induced by a large σ_{PGPE} relative to the chosen population sizes n_{ps} .

To assess the effect this practically has on PGPE training, we train for 50 epochs with different standard deviations σ_{PGPE} and present the results in Figure 9. As expected, we clearly observe that both too small and too large standard deviations lead to poor performance. However, and perhaps surprisingly, we find that training performance is relatively insensitive to the exact standard deviation as long as we are in the right order of magnitude between 10^{-3} and 10^{-2} .

4.3. Scaling to Deeper Networks

While the results presented so far are promising, they are obtained on relatively small networks. We now investigate how the effects of Gaussian Loss Smoothing via PGPE scale to deeper networks. In Table 3 we compare the performance of a CNN5 trained with PGPE + DEEPPOLY on MNIST at $\epsilon = 0.1$ to a range of GRAD-based training methods including the state of the art SABR (Müller et al., 2021) and STAPS (Mao et al., 2023a).

Table 3. Accuracies of a CNN5 on MNIST 0.1 depending on training method.

Training Method	Nat. [%]	Cert. [%]	Adv. [%]
IBP	96.67	93.02	93.04
SABR 0.1	98.60	94.87	94.95
STAPS 0.2	98.60	94.98	95.03
DEEPPOLY	88.82	84.34	84.35
DEEPPOLY-PGPE	98.83	96.98	97.08

Encouragingly, we not only observe that PGPE training improves performance significantly for the same bound computation method but that PGPE + DEEPPOLY dominates all other methods, substantially improving even over state-of-the-art GRAD-based methods. This result agrees well with our expectation that bound tightness becomes increasingly important with network depth, as in particular box approximation errors grow exponentially with the number of layers (Shi et al., 2021; Müller et al., 2023; Mao et al., 2023b).

5. Limitations

Unfortunately, training with PGPE, in particular in combination with DEEPPOLY, is prohibitively computationally expensive, preventing us from experimenting with larger architectures. In fact, training our CNN5 already required over 3 weeks on 8 V100s (> 4000 GPU hours translating to approximately \$10 000). We thus believe it is both an essential but also extremely promising item for future work to investigate more computationally efficient approaches for Gaussian Loss Smoothing in certified training.

6. Conclusion

We show that Gaussian Loss Smoothing can overcome the paradox of certified training by inducing a continuous and infinitely differentiable loss surface even for tight bound computation methods. To validate this empirically, we implement Gaussian Loss Smoothing via PGPE for certified training and demonstrate that, in this setting, tighter bounds lead to networks with strictly better performance. While our approach is computationally expensive, we believe it highlights a promising direction for future work and confirms the crucial importance of continuity and sensitivity in certified training.

7. Broader Impact

This paper presents work whose goal is to advance the field of Machine Learning. There are many potential societal consequences of our work, none of which we feel must be specifically highlighted here.

Acknowledgements

This work has been done as part of the EU grant ELSA (European Lighthouse on Secure and Safe AI, grant agreement no. 101070617) and the SERI grant SAFEAI (Certified Safe, Fair and Robust Artificial Intelligence, contract no. MB22.00088). Views and opinions expressed are however those of the authors only and do not necessarily reflect those of the European Union or European Commission. Neither the European Union nor the European Commission can be held responsible for them.

The work has received funding from the Swiss State Secretariat for Education, Research and Innovation (SERI).

This research was partially funded by the Ministry of Education and Science of Bulgaria (support for INSAIT, part of the Bulgarian National Roadmap for Research Infrastructure).

References

- Biggio, B., Corona, I., Maiorca, D., Nelson, B., Srndic, N., Laskov, P., Giacinto, G., and Roli, F. Evasion attacks against machine learning at test time. In *Proc of ECML PKDD*, 2013. doi: 10.1007/978-3-642-40994-3\25.
- Brix, C., Müller, M. N., Bak, S., Johnson, T. T., and Liu, C. First three years of the international verification of neural networks competition (VNN-COMP). *CoRR*, abs/2301.05815, 2023. doi: 10.48550/ARXIV.2301.05815.
- Croce, F. and Hein, M. Reliable evaluation of adversarial robustness with an ensemble of diverse parameter-free attacks. In *Proc. of ICML*, 2020.
- Ferrari, C., Müller, M. N., Jovanović, N., and Vechev, M. T. Complete verification via multi-neuron relaxation guided branch-and-bound. In *Proc. of ICLR*, 2022.
- Gehr, T., Mirman, M., Drachler-Cohen, D., Tsankov, P., Chaudhuri, S., and Vechev, M. T. AI2: safety and robustness certification of neural networks with abstract interpretation. In *Proc. of S&P*, 2018. doi: 10.1109/SP.2018.00058.
- Gowal, S., Dvijotham, K., Stanforth, R., Bunel, R., Qin, C., Uesato, J., Arandjelovic, R., Mann, T. A., and Kohli, P. On the effectiveness of interval bound propagation for training verifiably robust models. *ArXiv preprint*, abs/1810.12715, 2018.
- He, K., Zhang, X., Ren, S., and Sun, J. Delving deep into rectifiers: Surpassing human-level performance on imagenet classification. In *Proc. of ICCV*, 2015. doi: 10.1109/ICCV.2015.123.
- Jovanović, N., Balunović, M., Baader, M., and Vechev, M. T. On the paradox of certified training. *Trans. Mach. Learn. Res.*, 2022.
- Katz, G., Barrett, C. W., Dill, D. L., Julian, K., and Kochenderfer, M. J. Reluplex: An efficient SMT solver for verifying deep neural networks. *ArXiv preprint*, abs/1702.01135, 2017.
- Kingma, D. P. and Ba, J. Adam: A method for stochastic optimization. In Bengio, Y. and LeCun, Y. (eds.), *Proc. of ICLR*, 2015.
- Krizhevsky, A., Hinton, G., et al. Learning multiple layers of features from tiny images. 2009.
- Lange, R. T., Tang, Y., and Tian, Y. Neuroevobench: Benchmarking evolutionary optimizers for deep learning applications. In *Proc. of NeurIPS Datasets and Benchmarks Track*, 2023.
- LeCun, Y., Cortes, C., and Burges, C. Mnist handwritten digit database. *ATT Labs [Online]*. Available: <http://yann.lecun.com/exdb/mnist>, 2010.
- Mao, Y., Mueller, M. N., Fischer, M., and Vechev, M. Connecting certified and adversarial training. In *Proc. of NeurIPS*, 2023a.
- Mao, Y., Müller, M. N., Fischer, M., and Vechev, M. T. Understanding certified training with interval bound propagation. *CoRR*, abs/2306.10426, 2023b. doi: 10.48550/ARXIV.2306.10426.
- Mirman, M., Gehr, T., and Vechev, M. T. Differentiable abstract interpretation for provably robust neural networks. In Dy, J. G. and Krause, A. (eds.), *Proc. of ICML*, 2018.
- Müller, M. N., Balunović, M., and Vechev, M. T. Certify or predict: Boosting certified robustness with compositional architectures. In *Proc. of ICLR*, 2021.
- Müller, M. N., Eckert, F., Fischer, M., and Vechev, M. T. Certified training: Small boxes are all you need. In *Proc. of ICLR*, 2023.
- Palma, A. D., Bunel, R., Dvijotham, K., Kumar, M. P., and Stanforth, R. IBP regularization for verified adversarial robustness via branch-and-bound. *ArXiv preprint*, abs/2206.14772, 2022.
- Palma, A. D., Bunel, R., Dvijotham, K., Kumar, M. P., Stanforth, R., and Lomuscio, A. Expressive losses for verified robustness via convex combinations. *CoRR*, abs/2305.13991, 2023. doi: 10.48550/arXiv.2305.13991.
- Paszke, A., Gross, S., Massa, F., Lerer, A., Bradbury, J., Chanan, G., Killeen, T., Lin, Z., Gimelshein, N., Antiga, L., Desmaison, A., Köpf, A., Yang, E., DeVito, Z., Raison, M., Tejani, A., Chilamkurthy, S., Steiner, B., Fang, L., Bai, J., and Chintala, S. Pytorch: An imperative style, high-performance deep learning library. In *Proc. of NeurIPS*, 2019.
- Sehnke, F., Osendorfer, C., Rückstieß, T., Graves, A., Peters, J., and Schmidhuber, J. Parameter-exploring policy gradients. *Neural Networks*, 2010. doi: 10.1016/J.NEUNET.2009.12.004.
- Shi, Z., Wang, Y., Zhang, H., Yi, J., and Hsieh, C. Fast certified robust training with short warmup. In Ranzato, M., Beygelzimer, A., Dauphin, Y. N., Liang, P., and Vaughan, J. W. (eds.), *Proc. of NeurIPS*, 2021.
- Singh, G., Gehr, T., Mirman, M., Püschel, M., and Vechev, M. T. Fast and effective robustness certification. In *Proc. of NeurIPS*, 2018.

- Singh, G., Gehr, T., Püschel, M., and Vechev, M. T. An abstract domain for certifying neural networks. *Proc. of POPL*, 2019. doi: 10.1145/3290354.
- Starnes, A., Dereventsov, A., and Webster, C. Gaussian smoothing gradient descent for minimizing high-dimensional non-convex functions, 2023.
- Szegedy, C., Zaremba, W., Sutskever, I., Bruna, J., Erhan, D., Goodfellow, I. J., and Fergus, R. Intriguing properties of neural networks. In *Proc. of ICLR*, 2014.
- Toklu, N. E., Atkinson, T., Micka, V., Liskowski, P., and Srivastava, R. K. Evotorch: Scalable evolutionary computation in python, 2023.
- Tramèr, F., Carlini, N., Brendel, W., and Madry, A. On adaptive attacks to adversarial example defenses. In *Proc. of NeurIPS*, 2020.
- Wang, S., Pei, K., Whitehouse, J., Yang, J., and Jana, S. Efficient formal safety analysis of neural networks. In *Proc. of NeurIPS*, 2018.
- Weng, T., Zhang, H., Chen, H., Song, Z., Hsieh, C., Daniel, L., Boning, D. S., and Dhillon, I. S. Towards fast computation of certified robustness for relu networks. In *Proc. of ICML*, 2018.
- Wong, E. and Kolter, J. Z. Provable defenses against adversarial examples via the convex outer adversarial polytope. In *Proc. of ICML*, 2018.
- Zhang, H., Weng, T., Chen, P., Hsieh, C., and Daniel, L. Efficient neural network robustness certification with general activation functions. In *Proc. of NeurIPS*, 2018.
- Zhang, H., Chen, H., Xiao, C., Goyal, S., Stanforth, R., Li, B., Boning, D. S., and Hsieh, C. Towards stable and efficient training of verifiably robust neural networks. In *Proc. of ICLR*, 2020.
- Zhang, H., Wang, S., Xu, K., Li, L., Li, B., Jana, S., Hsieh, C., and Kolter, J. Z. General cutting planes for bound-propagation-based neural network verification. *ArXiv preprint*, abs/2208.05740, 2022.

A. PGPE Optimizes Smoothed Loss

Lemma A.1. *For any reasonably growing loss function $L(\theta)$ such that $|L(\theta)| \exp(-\theta^{2-\delta}) = O(1)$ for some $0 < \delta < 2$, let its Gaussian smoothing be $L_\sigma(\theta) = \mathbb{E}_{\epsilon \sim \mathcal{N}(0, \sigma^2)} L(\theta + \epsilon)$ for some $\sigma > 0$. Then $L_\sigma(\theta)$ is continuous and infinitely differentiable.*

Proof. $L_\sigma(\theta)$ exists due to the growth bound on $L(\theta)$. Further,

$$\begin{aligned} \frac{L_\sigma(\theta + \Delta\theta) - L_\sigma(\theta)}{\Delta\theta} &= \frac{1}{\Delta\theta} [\mathbb{E}_{\epsilon_1 \sim \mathcal{N}(\Delta\theta, \sigma^2)} L(\theta + \epsilon_1) - \mathbb{E}_{\epsilon_2 \sim \mathcal{N}(0, \sigma^2)} L(\theta + \epsilon_2)] \\ &= \int_{-\infty}^{\infty} \frac{1}{\Delta\theta} [P_{\epsilon_1}(x) - P_{\epsilon_2}(x)] L(\theta + x) dx \\ &= \int_{-\infty}^{\infty} \nabla_x \left[\frac{1}{\sqrt{2\pi\sigma^2}} \exp\left(-\frac{x^2}{2\sigma^2}\right) \right] L(\theta + x) dx \\ &= - \int_{-\infty}^{\infty} P_{\mathcal{N}(0, \sigma^2)}(x) L(\theta + x) \cdot \frac{x}{\sigma^2} dx. \end{aligned}$$

Since $|L(x)| \exp(-x^{2-\delta}) = O(1)$, the above integral is finite, thus $L_\sigma(\theta)$ has first-order derivative and continuous. Similarly, we can show that $L_\sigma(\theta)$ has higher-order derivatives and thus infinitely differentiable. \square

Lemma A.2. *If $L(\theta)$ is L -smooth, then $L_\sigma(\theta)$ is L -smooth as well.*

Proof. We cite this result from [Starnes et al. \(2023\)](#). \square

Lemma A.3. *PGPE approximately minimizes the smoothed loss $L_\sigma(\theta)$ by sampling. In particular, the expectation of the PGPE update on θ is the true gradient of $L_\sigma(\theta)$, i.e., $\mathbb{E} \nabla_\theta \hat{L}_\sigma(\theta) = \nabla L_\sigma(\theta)$.*

Proof. This follows from the design principle of PGPE. For more details, see [Sehnke et al. \(2010\)](#). \square

Corollary A.4. *The loss surface of PGPE is continuous, infinitely differentiable and more smooth than $L(\theta)$ for any reasonably growing loss function $L(\theta)$.*

Proof. This follows from Theorem A.1 and Theorem 3.1. \square

B. Additional Training Details

B.1. Standard Certified Training

We train with the Adam optimizer ([Kingma & Ba, 2015](#)) with a starting learning rate of 5×10^{-5} for 70 epochs on MNIST and 160 epochs on CIFAR-10. We use the first 20 epochs on MNIST and 80 epochs on CIFAR-10 for ϵ -annealing and we decay the learning rate by a factor of 0.2 after epochs 50 and 60 for MNIST and respectively 120 and 140 for CIFAR-10.

B.2. PGPE Training

We use a training schedule of 150 epochs, with a batch size of 512 for MNIST and 128 for CIFAR-10. We train with a starting learning rate of 0.0003 and we decay it twice by a factor of 0.4 after the 110th and 130th epoch. We use the first 50 epochs for ϵ -annealing only when training with the large value of ϵ for each dataset (MNIST $\epsilon = 0.3$ and CIFAR-10 $\epsilon = 8/255$).

B.3. Architectures

In Table 4 we present the two network architectures used for all our experiments.

Table 4. Network architectures of the convolutional networks for CIFAR-10 and MNIST. All layers listed below are followed by a ReLU activation layer. The output layer is omitted. ‘CONV c h×w/s/p’ corresponds to a 2D convolution with c output channels, an h×w kernel size, a stride of s in both dimensions, and an all-around zero padding of p.

CNN3	CNN5
CONV 8 5×5/2/2	CONV 16 5×5/2/2
CONV 8 4×4/2/1	CONV 16 4×4/2/1
	CONV 32 4×4/2/1
	FC 512

B.4. Dataset and Augmentation

We use the MNIST (LeCun et al., 2010) and CIFAR-10 (Krizhevsky et al., 2009) datasets, all of which are freely available with no license specified.

The data preprocessing mostly follows Müller et al. (2023). For MNIST, we do not apply any preprocessing. For CIFAR-10, we normalize with the dataset mean and standard deviation (after calculating perturbation size) and augment with random horizontal flips. In addition, we apply random cropping to 32 × 32 after applying a 2 pixel padding at every margin for CIFAR-10.

B.5. Training costs (Time and Resources)

In Table 5 we present a detailed analysis of the training costs of the PGPE method for all of our experimental settings.

Table 5. Training costs and workload distribution across GPUs / actors for each train setting.

Datset	Architecture	Relaxation	GPUs	Num. Actors	Time/epoch (min)	GPU-h/epoch
MNIST	CNN3	IBP	2 x L4	4	2.8	0.09
		SABR	2 x L4	4	7.6	0.25
		STAPS	2 x L4	4	17	0.57
		CROWN-IBP	2 x L4	4	8.5	0.28
		HBOX	8 x L4	8	31	4.13
		DEEPPOLY	8 x L4	8	27	3.60
		DEEPPOLY	8 x V100	8	16	2.13
	CNN5	DEEPPOLY	8 x L4	8	312	41.6
		DEEPPOLY	8 x V100	8	207	27.6
	CIFAR-10	CNN3	IBP	2 x L4	4	6.9
SABR			4 x L4	8	14	0.93
CROWN-IBP			4 x L4	8	8.5	0.57
DEEPPOLY			8 x V100	8	29	3.87

B.6. Train Dynamics

In Figure 10 we present the evolution of the Training Loss during training with different values for popsize n_{ps} . We observe significantly slower training as we decrease n_{ps} , confirming the theoretical prediction that using lower popsize decreases the quality of gradient estimations due to increased variance in the loss-sampling process.

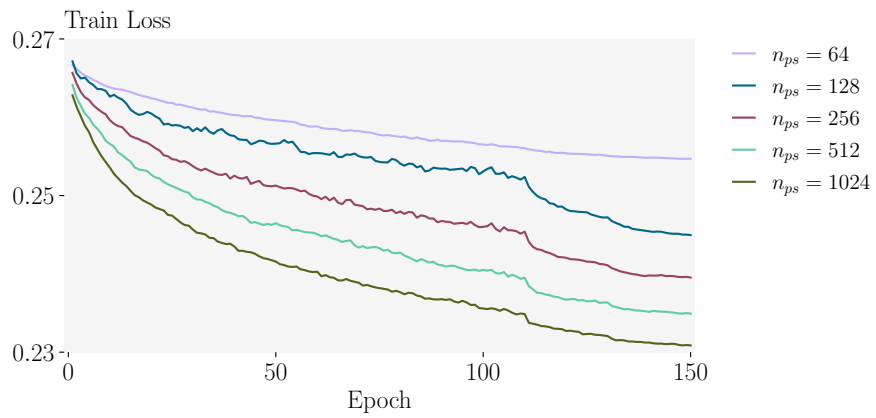


Figure 10. Evolution of Train Loss during training with different values for popsize n_{ps} . Note that for $n_{ps} = 64$ we trained with a lower learning rate because the value used in the other settings would make training unstable.